

THE LYNX-URSA MAJOR SUPERCLUSTER

RICCARDO GIOVANELLI

Arecibo Observatory,^{a)} Arecibo, Puerto Rico

MARTHA P. HAYNES

National Radio Astronomy Observatory,^{b)} Green Bank, West Virginia

Received 12 May 1982; revised 7 July 1982

ABSTRACT

The distribution of galaxies in the region of Lynx-Ursa Major outlines a filamentary structure which extends for approximately 3 h in right ascension, and is characterized by a surface number density contrast of about 3.7, on the average, with respect to its immediate surroundings. The average width of the filament is approximately 1.7 deg. Both the apparent magnitude distribution of the galaxies close to the filamentary enhancement and their redshift distribution indicate that the average redshift of the galaxies in the filament lies in the interval 4000–5300 km s⁻¹. Seventy-five newly determined 21-cm redshifts are presented and are used to complement the rest of the available redshift data to analyze the structure of the filament. We also point out the similarity of the redshift domain of the Lynx-Ursa Major filament with that of the Pisces-Perseus supercluster, from which it is separated by the width of the zone of avoidance; both the alignment of the filamentary axes and the significant preference of galaxies in that part of the zone of avoidance for the redshifts that characterize the two supercluster filaments are suggestive that Pisces-Perseus and Lynx-Ursa Major host two segments of a single connected superstructure that stretches from horizon to horizon.

I. INTRODUCTION

The assumption that the universe is homogeneous, when considered over large scales, has had a powerful influence on modern cosmology; it has usually been referred to as "the cosmological principle," and constitutes a formally pleasing statement on the nonuniqueness of man's place in the universe. If indeed such an assumption applies, the paramount question becomes, what is the threshold scale beyond which homogeneity occurs? The most widely accepted answer to that question is provided by the results of the correlation analysis of the distribution of galaxies, which sets the size of the largest clumps at about 20 Mpc (Peebles 1980). However, a glance at maps representing the number of counts of galaxies per unit area, projected on the celestial sphere, from relatively rich samples, suggests to the observer the existence of elongated structures which maintain an appearance of coherence over angles of tens of degrees; similarly, the distribution of redshifts over wide regions of sky often reveal pronounced clumping in relatively narrow redshift intervals and suggest the existence of large volumes of extremely rarefied galaxian

density (e.g., Chincarini, Rood, and Thompson 1981). The sizes of these irregularities appear to be in excess of 20 Mpc. Einasto, Jõeveer, and Saar (1980) have emphasized the existence of the Perseus supercluster, a filamentary structure with a length on the order of one radian at a redshift of about 5000 km s⁻¹.

We have searched for evidence of large-scale inhomogeneities in the local universe, as defined by the sample represented by the objects listed in the *Catalog of Galaxies and Clusters of Galaxies* (CGCG; Zwicky *et al.* 1963–1968). Comprising the largest compilation of galaxian positions and magnitudes, the CGCG is the best widely available source to study the possible existence of large angular size (say on the order of one radian), relatively nearby (radial velocities below $\sim 15\,000$ km s⁻¹) superstructures. We have then produced maps of the surface number density of CGCG galaxies over the part of the sky covered by such compilation, and identified a number of statistically significant extended structures; we then proceeded to study the velocity field of the regions occupied by those structures to verify whether morphological coherence extends to the redshift domain. In this paper we present the evidence that we have collected with regards to one of such structures, located in the Lynx-Ursa Major region which, although still fragmentary, suggests the existence of a coherent supercluster filament heretofore unrecognized.

II. GALAXY COUNTS

Figure 1 shows a Cartesian projection of a region of

^{a)} The Arecibo Observatory is part of the National Astronomy and Ionosphere Center, which is operated by Cornell University under contract with the National Science Foundation.

^{b)} The National Radio Astronomy Observatory is operated by Associated Universities, Inc., under contract with the National Science Foundation.

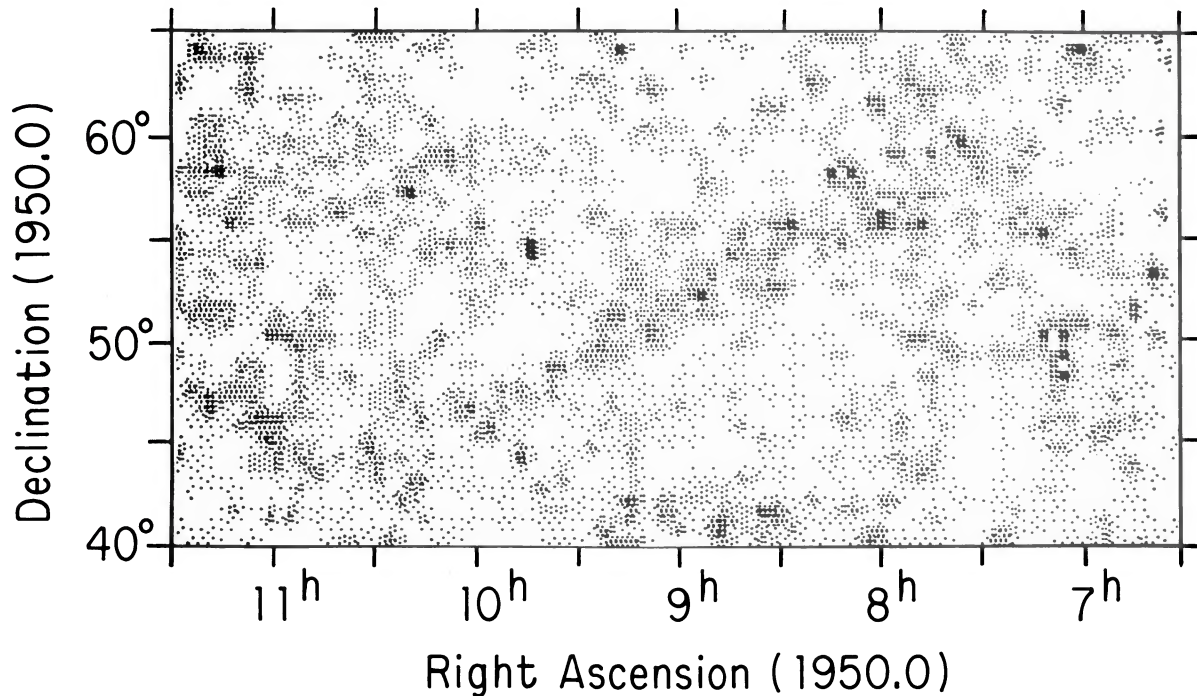


FIG. 1. Surface density distribution of galaxies in the CGCG. A quantity proportional to the logarithm of the density, averaged over cells of 3 min in R.A. and 0.5 degrees in Dec., is represented by an eight-level shade scale. The filamentary enhancement is more conspicuous between 7.5 and 10 h.

the sky engulfing mainly parts of the Lynx and Ursa Major constellations. The shade density is proportional to the logarithm of the number density of galaxies, averaged over cells of 3 min of time in right ascension by 0.5 deg in declination. The sample galaxies counted correspond to all the entries in the region from the CGCG. A filamentary density enhancement is discerned, running roughly in the direction northwest to southeast, more

conspicuous between 7.5 and 10 h. Between 8.33 and 10.10 h in right ascension, the filament's axis was fit by a straight line defined as

$$\delta_a = 106 - 6.0 \alpha_a, \quad (1)$$

where α_a and δ_a are the axis' coordinates in hours and degrees, respectively. An indication of the average density contrast between the filament enhancement and its surroundings is illustrated in Fig. 2, which was obtained in the following way. Strips of 20 deg stretched in the declination direction, and centered at δ_a , were binned every 10 arcmin; as the right ascension of the strip varies between 8.33 and 10.10 h, δ_a varies according to Eq. (1); galaxies of the CGCG were counted within each bin, characterized by a declination distance from the filament's axis, $\delta - \delta_a$. The profile of Fig. 2 is then the average number of galaxies $n(|\delta - \delta_a|)$ folded around $\delta = \delta_a$. The smooth curve superimposed on the histogram is a Gaussian fit to the distribution: the Gaussian baseline stands at 6.8 counts, while its peak is at 25.4, and the full width at half peak intensity is 2 deg. We hence derive an average surface number density contrast of 3.7:1 and an average width perpendicular to the axis of about 1.7 deg, for the filament.

If the enhancement in the surface density of galaxies represents a true increase in the space density of galaxies within a relatively narrow interval of distances from us, one should expect to find some indication of the enhancement by analyzing the distribution of apparent

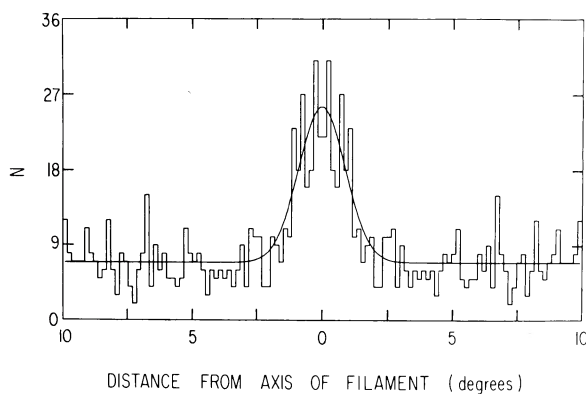


FIG. 2. Illustration of the surface density contrast in the filament shown in Fig. 1. Defining the filamentary axis as per Eq. (1) in the text, the ordinate represents the number of galaxy counts, in the CGCG, within bins of 10 arcmin in Dec. and over the range 8.33 to 10.10 h of R.A., as a function of distance measured in the North-South direction from the filament's axis. The profile is folded around $|\delta - \delta_a| = 0$ and a Gaussian fit is represented by the smooth curve.

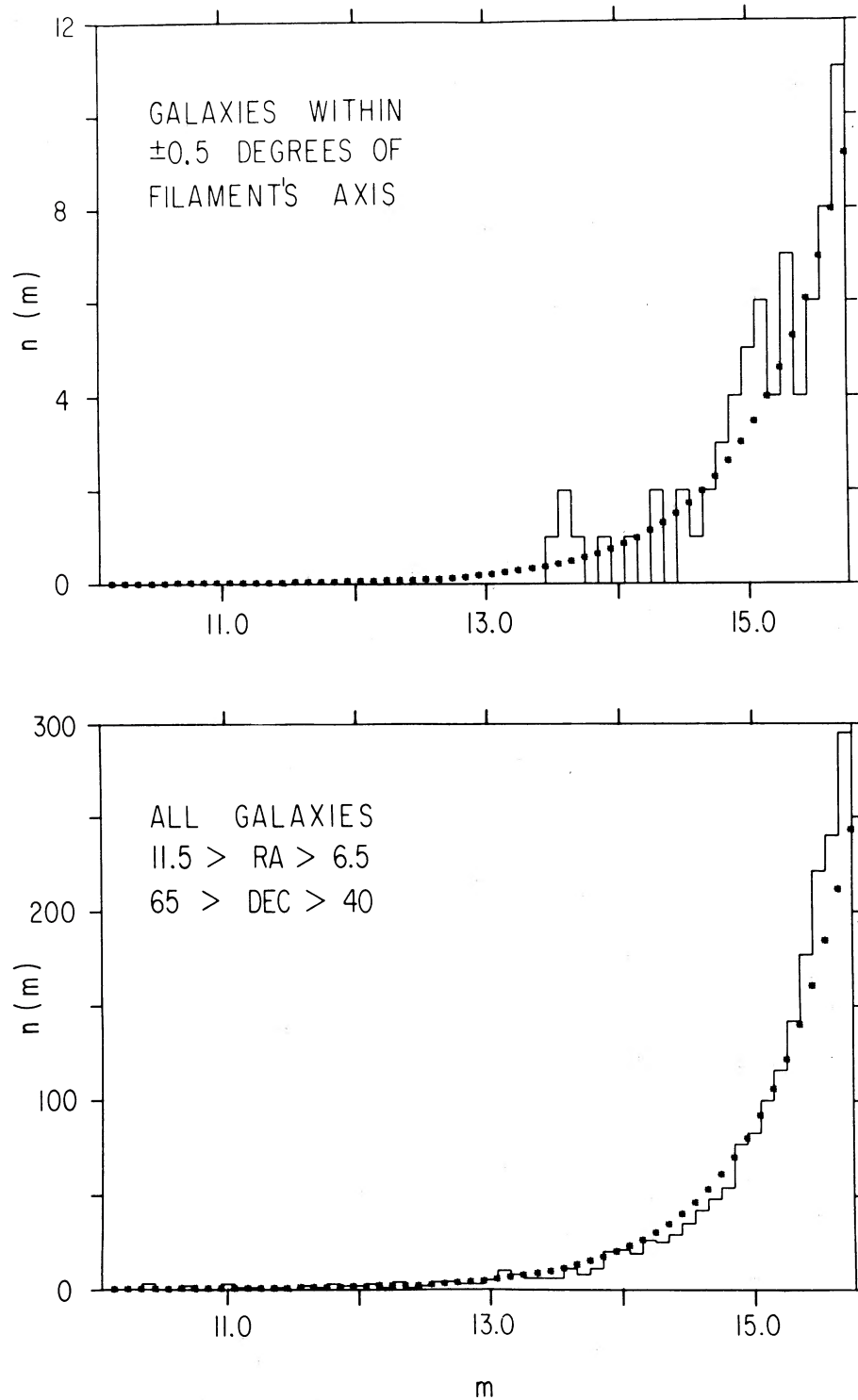


FIG. 3. Galaxy counts per apparent magnitude bin $n(m)$, from the CGCG. Panel (a) includes only those galaxies within a strip one degree wide centered along the axis of the filament as defined by Eq. (1), while panel (b) includes all the CGCG galaxies within the region displayed in Fig. 1. The smooth curves outlined by asterisks represent the expected $n(m)$ for a uniformly distributed galaxian population. Notice the excess between $m = 14.9$ and $m = 15.3$ in panel (a).

magnitudes in the region of the filament. The reasoning proceeds as follows. Let $\phi(M)dM$ represent the galaxian luminosity function, i.e., the number of galaxies with absolute magnitude between M and $M + dM$. As a first order approximation, assume that $\phi(M)$ is independent of the spatial location of the sample, and will be the same in regions of relatively enhanced galaxian density, which may be the case within the filament, as in the more rarefied regions in its foreground and background. Then, the number of galaxies with an apparent magnitude between m and $m + dm$, located at a distance interval $r, r + dr$ within a solid angle $\Delta\Omega$, is

$$n(m,r)dr dm \Delta\Omega = D(r)\phi[m - 5 \log(r/10)]\Delta\Omega r^2 dr dm, \quad (2)$$

where $D(r)$ is the space density of galaxies, which in this instance we shall consider just a function of the distance r . Integrating over r , we obtain the number counts that would be expected for any complete, magnitude limited sample:

$$n(m)dm = n_0 \int_0^\infty \phi[m - 5 \log(r/10)]D(r)r^2 dr dm, \quad (3)$$

where n_0 is a normalization constant. "Slices" across the cone subtended by $\Delta\Omega$ at different distances r from the observer, sample different domains of the luminosity function, each weighted by $r^2 D(r)$. Observed galaxian luminosity functions are characterized by the presence of a "knee" at some characteristic absolute magnitude M^* , where the slope of $\phi(M)$ becomes substantially less steep for $M > M^*$. Hence, if some regions along the line of sight at a distance r' are affected by a large increase of $D(r)$, $n(m)$ should reflect such an increase by an excess around the bin for which $m' = M^* + 5 \log(r'/10)$. We have adopted a Schechter (1976) luminosity function

$$\phi(M)dM = \phi_0 10^{-0.4(M - M^*)(\alpha + 1)} \times \exp[-10^{-0.4(M - M^*)}]dM, \quad (4)$$

with $M^* = -20.6$ and $\alpha = -1.25$ (for blue magnitudes and a value of the Hubble constant of $50 \text{ km s}^{-1} \text{ Mpc}^{-1}$, which shall be used throughout this paper), and ϕ_0 a normalization constant.

Figures 3(a) and 3(b) display two sets of counts $n(m)$; for Fig. 3(a) only those galaxies in the CGCG were chosen that are contained within a strip 1 deg wide centered along the axis of the filament as defined by Eq. (1), and extending from 8.33 to 10.10 h in right ascension. Figure 3(b) includes all the CGCG galaxies within the region displayed in Fig. 1. Superimposed on each histogram is a smooth function, outlined by asterisks, representing the expectation derived from Eq. (3) after replacing $\phi(M)$ with Eq. (4), assuming $D(r) = \text{constant}$, and normalizing its integral between $m = 10.0$ and 15.7 to the area under the histogram. An excess is prominent in the observed histogram in Fig. 3(a), between $m = 14.9$ and 15.3 ; such excess occurs both with respect to the distribution ex-

TABLE I. Newly determined 21-cm heliocentric radial velocities.

UGC	V_0	UGC	V_0	UGC	V_0
2939	4443	3487	5211	5034	3210
3025	4985	3511	3567	5157	4841
3042	3059	3532	6287	5237	4684
3043	7400	3576	5948	5283	4658
3052	4242	3679	5832	5296	1520
3108	3961	3724	5925	5327	2994
3139	6290	3734	969	5354	1172
3167	4735	3799	5932	5389	6982
3217	4074	3828	3217	5534	7650
3218	5223	3885	3805	5698	8707
3245	4875	3922	8770	5791A	858
3250	4532	3933	5894	5791B	1517
3277	5115	3998	989	5888	1239
3284	4697	4027	5672	6009	1911
3314	2182	4043	3402	6069	6667
3325	6692	4176	3086	6096	2994
3346	5958	4226	7911	6228	3054
3354	3085	4380	7487	6257	5336
3375	5783	4415	3611	6266	2204
3382	4495	4445	6330	6275	1969
3394	1821	4515	4974	6335	2927
3403	1264	4659	1749	6385	1587
3418	6743	4807	3956	6390	1008
3436	4297	4824	2185	6416	1932
3477	6494	4867	2497	6484	2429

pected from a constant galaxian space density and to the observed average distribution shown in Fig. 3(b). Allowing for an average extinction of about 0.55 mag, the average extinction computed separately for 35 spiral galaxies located between 7.6 and 10.6 h in R.A. within the region outlined in Fig. 1 is 0.58 ± 0.30 ; this includes a component of galactic extinction computed following the suggestions of Burstein and Heiles (1978), and one of internal extinction, averaged over all inclinations and spiral types—the excess suggests a density enhancement at a redshift

$$v' = r'H = 10^{-5} \times 10^{0.2(15.1 - 0.55 - M^*)} \\ H = 5300 \text{ km s}^{-1}. \quad (5)$$

To this calculation we should attach the weight that corresponds to the relatively poor statistics of the histogram of Fig. 3(a). It provides, however, circumstantial evidence for the relatively nearby nature of the filamentary structure, one that may be confirmed with not great difficulty by using the redshifts available in the region.

III. REDSHIFT DISTRIBUTION

The next step in our analysis consists in verifying whether evidence of connectiveness exists in the redshift domain that may corroborate the tentative picture of a coherent filamentary superstructure brought forth in the preceding section. To that end, we have collected all the redshifts available for galaxies within the region of interest, using the compilation privately circulated by H. Rood (1981). To complement that set of data, we utilized redshifts newly obtained by us, the result of an ongoing survey being carried on at the 300-ft telescope of the National Radio Astronomy Observatory in Green Bank, West Virginia, in the 21-cm line. All the para-

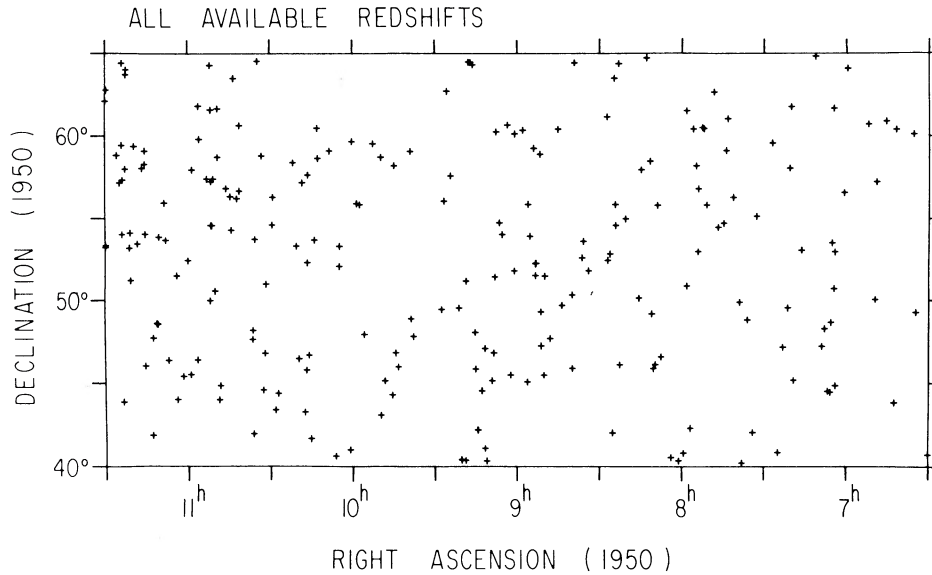


FIG. 4. Distribution of all galaxies with available redshift in the Lynx-Ursa Major region.

eters derived from the observations will be given for the whole sample in another paper; here, we shall limit ourselves to list the heliocentric radial velocities of 75 galaxies among those observed, which will be used in the following analysis. They are listed in Table I, where each entry is identified by its ordinal number in the Uppsala General Catalog of Galaxies (Nilson 1973).

Figure 4 shows the distribution of all galaxies with available redshift in the region of interest, while Fig. 5 is limited to those galaxies whose redshifts are between 3000 and 5300 km s^{-1} . Although Fig. 4 illustrates the relative lack of spatial bias of the sample of all available redshifts, in the sense that no obvious "over representation" of galaxies outlining the filament is evident, significant crowding toward the narrow region outlined by the density enhancement in the galaxy counts is present in Fig. 5. Two-thirds of all galaxies in Fig. 5 are within 2.5 deg from the ridge defined by the filament's maxi-

mum surface density regions, the filamentary structure itself appearing rather conspicuous in this figure alone. This result reinforces the evidence collected in Sec. II, but we would like to investigate somewhat the biases present in the sample of galaxies with available redshifts. While the spatial segregation of galaxies observed in Fig. 5 appears rather striking, are there any differences in the characteristics of the sample of galaxies with known redshift that lie close to the filament from those that do not that may favor their being found in the velocity window 3000–5300 km s^{-1} ?

In order to answer that question, we have separately analyzed two samples: one includes all the galaxies plotted in Fig. 4, the second is a subsample of the first, limited to those objects located within 5 deg of the filamentary axis as defined by Eq. (1) in the preceding section. A magnitude distribution histogram $n(m)$, sampled in bins of 0.1 mag was constructed for each sample. From such

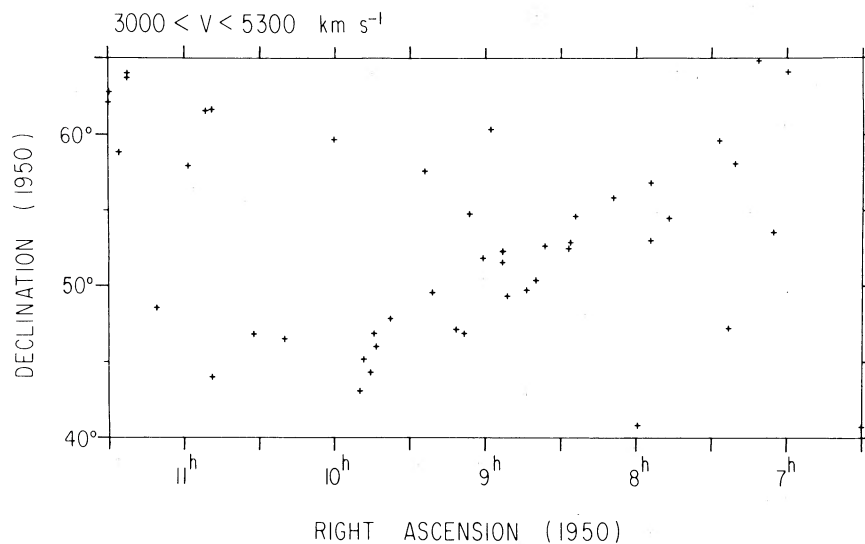


FIG. 5. Subset of the galaxies shown in Fig. 4 limited to redshifts between 3000 and 5300 km s^{-1} .

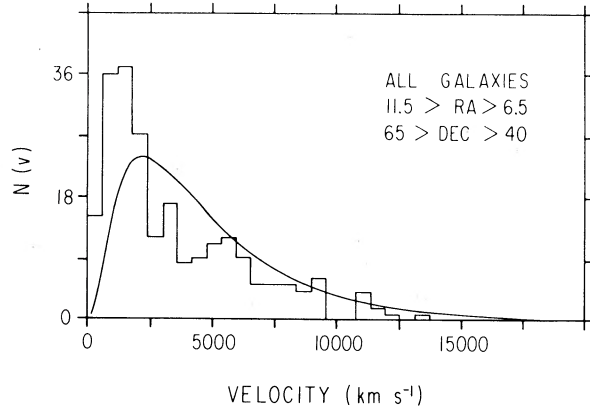


FIG. 6. Redshift histogram of all galaxies with available redshift (same as in Fig. 4), binned every 600 km s^{-1} . The smooth curve superimposed represents the expected z distribution of the sample if it were uniformly distributed in space and characterized by a Schechter's luminosity function. The excess at low redshifts is a signature of the Local Supercluster.

a magnitude distribution one can derive an *expected* redshift distribution on the assumptions that the galaxies are well represented by a Schechter luminosity function and a constant space density to be compared with the observed redshift distribution. We can proceed as follows: we can rewrite Eq. (2) in Sec. II as

$$N(v, m) dv dm \Delta\Omega = D \left(\frac{v}{H} \right) \phi \left[m - 5 \log \left(\frac{v}{10H} \right) \right] \times \Delta\Omega \left(\frac{v}{H} \right)^2 d \left(\frac{v}{H} \right) dm, \quad (6)$$

which gives the number of galaxies with redshift between v and $v + dv$, and the apparent magnitude between m and $m + dm$, within the solid angle $\Delta\Omega$. To

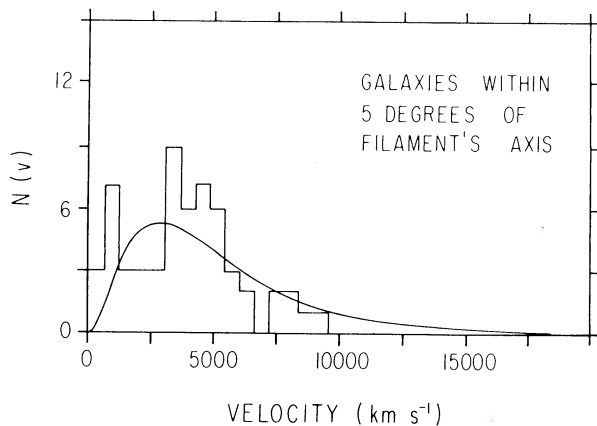


FIG. 7. Histogram of the galaxies with available redshifts contained within 5 deg of the filament's axis as defined by Eq. (1). The smooth curve represents the expected z distribution as described in the caption to Fig. 6.

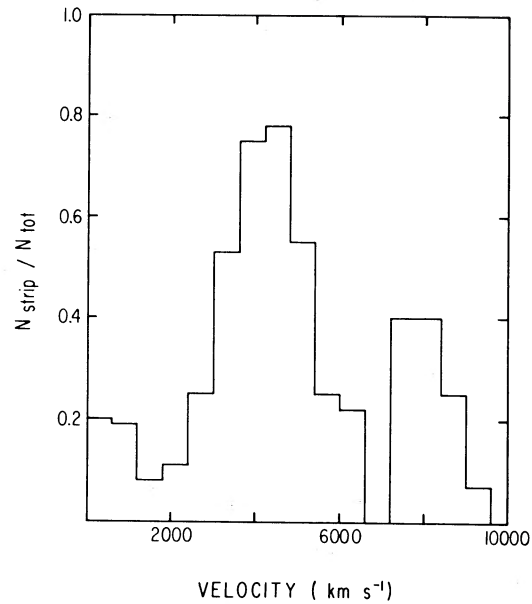


FIG. 8. Ratio of the number of galaxies within a strip 10° wide centered around the filamentary axis to that of galaxies in the whole surveyed area enclosed in Fig. 1, in 600 km s^{-1} bins.

obtain the redshift distribution of a complete sample limited to magnitudes m brighter than m_2 , we should integrate Eq. (6) in dm , up to m_2 . If our sample is not complete, we can compute its degree of completeness for each value of m , by comparing its observed apparent magnitude distribution $n(m) dm$ with that of a complete sample: taking the ratio of the two, we can obtain a "completeness function" $c(m)$. We may then estimate the expected redshift distribution of our incomplete sample by computing

$$N(v) dv = dv \int N(v, m) c(m) dm. \quad (7)$$

Figures 6 and 7 show the results of the calculation described by Eq. (7) as smooth curves, separately for the two samples defined above. Superimposed on each figure is the histogram of observed radial velocities, binned in intervals of 600 km s^{-1} . The area under the smooth curve and under the histogram are the same. Figure 6 shows an excess of galaxies at velocities below 2000 km s^{-1} , the effect of contamination of the sample by galaxies belonging to the local supercluster. A trace of that contamination is also present in Fig. 7, although there the most conspicuous feature is the excess in the velocity range $3000\text{--}5300 \text{ km s}^{-1}$, which provides completely independent evidence from that obtained in Sec. II, that an enhancement of the spatial density $D(r)$ exists in the region of the filament at a distance corresponding to a redshift in the neighborhood of 5000 km s^{-1} . Yet another form of showing the contrast between the velocity distribution of the main sample represented in Figs. 4 and 6 and the subsample represented by the galaxies

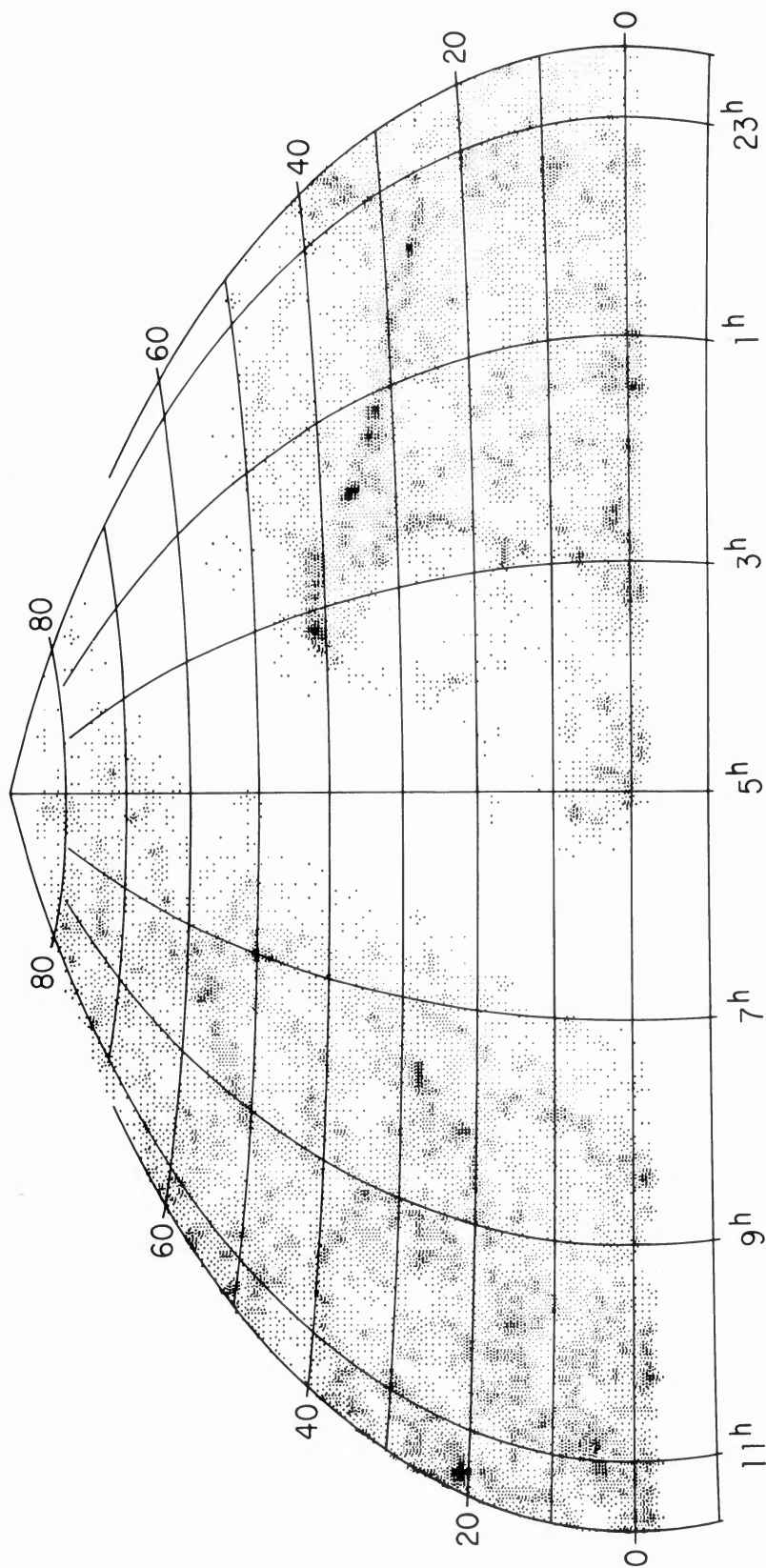


FIG. 9. Shade density plot analogous to Fig. 1, except that the cell size is here one square degree and the celestial sphere has been forced into an Aitoff (equal area) projection. The set of filaments between 23 and 3.5 h is the Perseus-Pisces supercluster. The unshaded band coming from NW to SE is the zone of avoidance.

binned in Fig. 7 is shown in Fig. 8. For each velocity bin we plot the ratio of the number of galaxies within 5° of the filament to that in the whole surveyed area. The prominent peak centered near 4200 km s^{-1} is identified with the filamentary density enhancement. The number of available redshifts belonging to the proposed filamentary structure's domain are still too scarce to attempt a meaningful measurement of the velocity dispersion of galaxies in the structure and hence of its three-dimensional shape.

IV. CONNECTION WITH THE PISCES-PERSEUS SUPERCLUSTER?

The existence of coherent supercluster chains with sizes well in excess of 20 Mpc has gained much credibility in recent years. Possibly the most spectacular in the local universe is constituted by the Pisces-Perseus chain, which extends over more than one radian in the southern galactic hemisphere. Its main part can be appreciated as the linear density enhancement extending between approximately R.A. = 23^{h} , Dec = 25° and R.A. = $3^{\text{h}}5$, Dec = 43° in the shade plot shown in Fig. 9, which was constructed with the same procedure followed for Fig. 1 using the CGCG, except that the pixel size is one square degree and the projection is of the Aitoff kind (equal area), to facilitate tracing features at high declination. The nature of the Perseus-Pisces supercluster has been emphasized by Einasto *et al.* (1980); their suggestion that this is an extended coherent feature is confirmed by the results of an H I survey of 1500 galaxies in the supercluster now reaching completion at the Arecibo Observatory, by Giovanelli, Haynes, and Chincarini. The unshaded band crossing the central parts of Fig. 9 is of course the consequence of the heavy extinction produced by the plane of our own galaxy.

One notices with interest that only 35° separate the Perseus region where the Pisces-Perseus chain merges into the zone of avoidance and the region where the Lynx-Ursa Major chain appears to do the same on the opposite side; the direction of the ideal segment connecting both of these regions coincides with that of the main axis of the Pisces-Perseus chain. Furthermore, the average velocity of galaxies in the Perseus region of the Pisces-Perseus chain is in the range $4500\text{--}5000 \text{ km s}^{-1}$, curiously close to that found in the Lynx-Ursa Major chain. These suggestions motivate the suspicion that the two complexes may be connected across the zone of avoidance, making extremely valuable redshifts obtainable in that region. However, few are available from the literature, as few, in fact, are the galaxies cataloged in the region at all. For those, 21-cm measurements provide the fastest means to obtain redshift information; in Table I a number of such redshifts are listed, and we plan to substantially increase the available number in the near future. Utilizing the available material we have produced Fig. 10, an attempt at analyzing the characteristics of the redshift distribution of the galaxies in the zone of avoidance. The sampled region was limited to

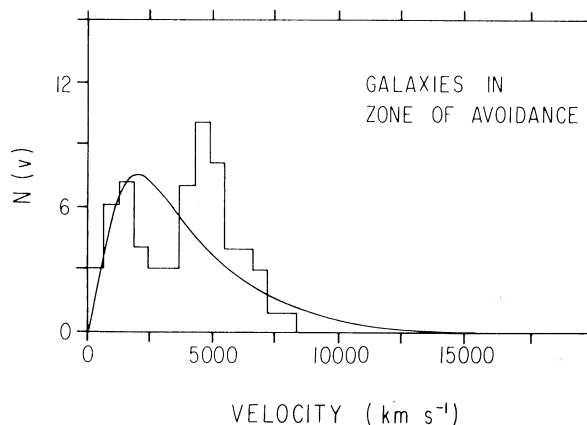


FIG. 10. Histogram of redshifts in the region of the zone of avoidance between the Perseus-Pisces and the Lynx-Ursa Major chains. The smooth curve represents the expected z distribution of the sample if the galaxies were uniformly distributed in space, characterized by Schechter's luminosity function and obscured by an average of 1.5 magnitudes.

$$6^{\text{h}}5 > \text{R.A.} > 4^{\text{h}}, \\ + 75^\circ > \text{Dec} > + 30^\circ.$$

The expected z distribution, represented by the smooth curve, was computed following the procedure outlined in Sec. III, and allowing for an average extinction of 1.5 mag. The histogram of observed redshifts shows a conspicuous excess between 3800 and 6800 km s^{-1} , further contributing to the suspicion of connectiveness between the Pisces-Perseus and the Lynx-Ursa Major chains.

If indeed Pisces-Perseus and Lynx-Ursa Major represent two segments of one connected structure, joint across the zone of avoidance, its angular extent would be on the order of three radians, or a few hundred Mpc. The structure would extend literally from horizon to horizon. The implications of such a result are sufficiently important to advise much caution and to recommend substantial improvement of the somewhat fragmentary statistical quality of the available observational material.

The picture offered by Fig. 9, and by similar representations covering other parts of the northern sky, is suggestive of the fact that filamentary structures seem to be the rule rather than the exception, in the distribution of galaxies in the local universe sampled by the CGCG. A filament-like density enhancement seems to connect the Hercules group of clusters, near R.A. $\approx 16^{\text{h}}$, Dec $\approx 17^\circ$, with the region dominated by the Abell clusters A2197/A2199, more than 20° to the north; Chincarini *et al.* (1981) have shown the velocity field of that region to be dominated by a strong clumping around the average redshift of both groups of clusters, near 11000 km s^{-1} . Similarly, from Hercules toward the South, in the region dominated by the nearby cluster centered on NGC 5846, filamentary structures are discerned and, again,

the Hercules velocity domain can be traced down to that region, 20° to the southwest of the Hercules clusters (Haynes and Giovanelli 1981). In Fig. 9 a linear chain is suggested between $7^{\text{h}}5$ and 10^{h} , running northwest to southeast and crossing $\text{Dec.} = 20^\circ$ near $\text{R.A.} = 9^{\text{h}}$, which engulfs the Cancer cluster. A preliminary analysis based on the data available in that region cannot support much speculation as the available redshifts, except in the region of the Cancer cluster, are few. We have shown elsewhere that even if one chooses a sample of galaxies as remote as possible from regions of enhanced galaxian density, such as clusters, groups, or filaments, the redshift distribution of those objects bears clear signature of the nearest supercluster structure over regions as extended as 2 or 3 sr (Haynes and Giovanelli 1982), drastically deviating from the expectations derived from a uniform space density of galaxies. These results lend credibility to a picture of the local universe dominated by very large scale inhomogeneities, that have characteristic linear sizes in excess of 100 Mpc. The cosmological principle seems to be applicable on scales no smaller than that.

Such large scale deviations from homogeneity may clearly be responsible for substantial deviations from isotropy, when redshift samples are utilized that represent volumes of space of linear sizes of 100 Mpc or less. Whether the widely publicized disagreements between the direction of motion of the Local Group with respect to the microwave background and with respect to a sample of relatively nearby Sc galaxies (Rubin *et al.* 1976) may be clarified by taking into account the scale of inhomogeneities remains a desirable task to tackle ahead.

V. CONCLUSIONS

We bring attention to an extended enhancement of the number density of galaxies in the Lynx-Ursa Major region, which is characterized by linear morphology and extends for approximately 3 h in R.A. at intermediate northern declinations. The average surface number density enhancement of the filament is of a factor of 3.7 with respect to its immediate surroundings, and has an average annular width, projected on the plane of the sky, of approximately 1.7 deg.

The apparent magnitude distribution of galaxies close to the filamentary axis shows an enhancement near $m = 15.1$, which, if interpreted as the knee of the galaxian luminosity function of the density enhancement corresponding to the filament, would predict for it a redshift of about 5300 km s^{-1} .

The galaxies with available redshift over the broad region that engulfs the filament manifest a marked preference for location near the filamentary axis, in the velocity window from 3000 to 5300 km s^{-1} , in the sense that when one plots the sky distribution of the galaxies within that velocity window, the outline of the filament emerges remarkably clear. Conversely, the observed redshift distribution of all galaxies close to the filament's axis shows a significant excess with respect to the redshift distribution that would be expected for a sample of galaxies with the same apparent magnitude distribution and a uniform space density; the excess occurs in the velocity range from 3000 to 5300 km s^{-1} .

These effects constitute strong evidence for the possibility that the Lynx-Ursa Major filament is a coherent supercluster structure similar in character, and in average distance, to the Pisces-Perseus supercluster. The traceability of both of those two filamentary structures wanes as they merge into the zone of avoidance, from opposite sides of the galactic plane, at a distance from each other of about 35 deg. The main axis of the better developed Pisces-Perseus feature is aligned as the direction defined by a linear connection between the two structures. Furthermore, the redshifts available for heavily obscured galaxies in the region of the zone of avoidance separating Perseus from Lynx is evidence a significant preference for the domain common to the two supercluster filaments, well in excess of the fraction of redshifts expected in that region from a uniformly distributed sample of galaxies. The suggestion that the two filaments are connected, forming a coherent structure which stretches over three radians is a strong motivation to improve the data base, a goal which we are pursuing by means of 21-cm line measurements.

We are grateful to an anonymous referee for helpful comments, including the suggestion of Fig. 8.

REFERENCES

- Burstein, D., and Heiles, C. (1978). *Astrophys. J.* **225**, 40.
 Chincarini, G. L., Rood, H. R. and Thompson, L. A. (1981). *Astrophys. J. Lett.* **249**, L47.
 Einasto, J., Jõeveer, M., and Saar, E. (1980). *Mon. Not. R. Astron. Soc.* **193**, 353.
 Haynes, M. P., and Giovanelli, R. (1981). *Bull. Am. Astron. Soc.* **13**, 842.
 Haynes, M. P., and Giovanelli, R. (1982). In preparation.
 Nilson, P. (1973). *Uppsala General Catalog of Galaxies*, Uppsala Astron. Obs. Ann. Band 6, Ser. V:A, Vol. 1 (UGC).
 Peebles, P. J. E. (1980). *Large Scale Structure of the Universe* (Princeton University, Princeton).
 Rood, H. R. (1981). Private communication.
 Rubin, V. C., Thonnard, N., Ford, W. K., and Roberts, M. S. (1976). *Astron. J.* **81**, 687.
 Schechter, P. (1976). *Astrophys. J.* **203**, 297.
 Zwicky, F., Herzog, E., Wild, P., Karpowicz, M., and Kowal, C. T. (1961–1968). *Catalog of Galaxies and Clusters of Galaxies* (California Institute of Technology, Pasadena), Vols. 1–6. (CGCG).